Research Square

Preprints are preliminary reports that have not undergone peer review. They should not be considered conclusive, used to inform clinical practice, or referenced by the media as validated information.

Spatiotemporal Dynamics and Assess of Ecological Quality in Sylhet Metropolitan Area amid Rapid Urbanization: A Remote Sensing Approach

Md Saikoth Jahan

md_saikoth.jahan@mailbox.tu-dresden.de

Technische Universität Dresden

Mst Arjumoni Anu

Technische Universität Dresden

Md. Inzamul Haque

Islamic University

Most. Atia Parvin

Islamic University

Research Article

Keywords: Urbanization, Ecological Quality, Sylhet Metropolitan Area, Spatiotemporal Dynamics, LEI, CEEI

Posted Date: October 20th, 2026

DOI: https://doi.org/10.21203/rs.3.rs-11422676/v1

License: This work is licensed under a Creative Commons Attribution 4.0 International License. Read Full License

Additional Declarations: No competing interests reported.

Spatiotemporal Dynamics and Assess of Ecological Quality in Sylhet Metropolitan Area amid Rapid Urbanization: A Remote Sensing Approach

ABSTRACT

The rapid urbanization of Sylhet, a major city in Bangladesh, has led to significant ecological challenges. This study evaluates the spatiotemporal dynamics of ecological quality in the Sylhet Metropolitan Area from 2003 to 2023 using a Comprehensive Ecological Evaluation Index (CEEI) derived from remote sensing data. The CEEI incorporates multiple remote sensing-based parameters such as the Normalized Difference Vegetation Index (NDVI), Land Surface Temperature (LST), and Vegetative Health Index (VHI), which together provide a robust assessment of the region's ecological conditions. The results indicate a general decline in ecological quality over the study period, with significant degradation occurring in urban areas. Despite some areas showing signs of ecological recovery, the overall trend suggests that the environmental pressures associated with urbanization are outpacing efforts to mitigate them. The results revealed that the changes in ecological quality displayed a pattern of improvement from 2003 to 2011, then degraded from 2011 to 2023, and the regions with poor and fair ecological quality gradually shifted from suburbs to urban areas. The urbanization process and policy variation mainly drove the changes in ecological quality, and these results may provide helpful information for ecological conservation and sustainable development of Sylhet.

Keywords: Urbanization, Ecological Quality, Sylhet Metropolitan Area, Spatiotemporal Dynamics, LEI, CEEI

1. Introduction

Urbanization is a global phenomenon that significantly impacts environmental quality, and some undesirable effects of rapid urbanization on ecology include the loss of green areas, increased pollution, and changing land use patterns. Sylhet is one of Bangladesh's major cities that is facing these challenges (Rahman *et al*., 2012). Sylhet has been undergoing extreme urbanization recently, with very high ecological consequences (Abdullah *et al*., 2022). This transition of the city leads to the conversion of natural land covers, such as forests and wetlands, into buildup areas. This process degrades local ecosystems and reduces ecological biodiversity (Seto *et al*., 2012). The causes of ecological quality degradation are complex in some specific study areas that may have very high human activity, similar to a city (Ba *et al.*, 2019). Over the last 20 years, Sylhet has undergone substantial changes in land use and cover (Kadir *et al*., 2021). Natural ecologically rich areas are

transformed into urban regions when cities grow, which results in a loss of natural population and biodiversity (Seto *et al*., 2012). Urbanization and ecology are closely interconnected because an imbalanced urbanization process is the prime cause of ecological deterioration (Liu *et al*.,2014). Rahman & Alam (2016) found a link between urbanization and ecology and suggested that urbanization can significantly harm local ecology. Islam *et al*. (2020) also used remote sensing to examine how urbanization affects ecosystem services' value. They suggested an enhanced ecological evaluation for more accurate and dependable results that can be applied to urban planning. Many studies have been undertaken focusing on different remote sensing (RS)- based indices to understand a city's ecological condition. For example, Fern *et al*. (2018) used NDVI to evaluate ecological changes based on green vegetation cover. However, the study concluded that NDVI could not accurately reflect the health condition of vegetation. A single indicator has limited explanatory power for the ecological environment quality because it ignores the contribution of other ecological environmental factors, while a comprehensive indicator can reveal more features related to the ecological environment quality (Yu *et al*.,2019). Additionally, the monitoring period should be extended to reveal ecological quality effectively. Therefore, it is necessary to improve the parameter selection and integration for an accurate assessment of ecology using remote sensing technology (Song & Xue, 2016; Yi *et al*.,2019). In 2015, the Ministry of Environmental Protection of China proposed the Ecological Environment Index (EI), which is calculated by the weighted summation of six indexes: the biological richness index, vegetation coverage index, water network denseness index, land stress index, pollution load index, and environmental restriction index. It is suitable for evaluating the ecological environment quality at the county level. However, selecting EI indicators is not rational in the native environment, and the setting of indicator weights is not objective. The calculated result is a numerical value, which cannot describe the spatial distribution of ecological environment quality. Indicators of ecological condition cannot be the same for every area, and their uneven contribution should be measured to evaluate ecological condition more precisely (Austin *et al*.,2007). Recent studies have used indicators based entirely on remote sensing, integrated various indicators using principal component analysis (PCA), and automatically assigned weights based on the contribution of each indicator to each principal component, thereby constructing a comprehensive evaluation index. For example, Xu *et al*. (2020) proposed the remote-sensing ecological index (RSEI) based on the four indicators of greenness, wetness, dryness, and heat to evaluate and predict the ecological conditions of the Xiong'an New

Area. Zhu *et al*. (2024) integrated soil-adjusted vegetation index (SAVI), normalized difference moisture index (NDMI), normalized difference soil index (NDSI), and normalized difference build-up index (NDBI) to establish integrated ecological index (IEI), which reflects the surface ecological conditions and thermal environmental effects of Xi'an in the past 20 years. Furthermore, Yang *et al*. (2024) integrated vegetative cover (VC), vegetative health index (VHI), normalized differential build-up, and bare soil index (NDBSI), land-surface moisture (LSM), and land-surface temperature (LST) to construct a comprehensive ecological evaluation index (CEEI), which reveals the impact of the urbanization movement from 1987 to 2017 on the ecological quality of Guangdong–Hong Kong–Macau Greater Bay Area (GBA) of China. Although the existing comprehensive evaluation indicators based on remote sensing are often used to evaluate the ecological environment quality for urban areas. The Remote Sensing Ecological Index (RSEI) is another dependable, widely used, and intriguing index to evaluate a city's ecological condition. It provides fast and accurate data on changes in land cover by integrating several parameters to produce a comprehensive picture of ecological quality (Xu *et al*., 2020). Studies have indicated that RSEI is a valuable tool for evaluating ecological conditions in places that are quickly urbanizing and can offer essential insights into the effects of urbanization (Geng *et al*., 2022). However, the cities of Bangladesh are unique and cannot be compared with European cities. Despite the heavy population, the cities of Bangladesh are moderately high-rise in nature (Ahsan *et al*., 2016). Buildings and infrastructures could be better planned and dispersed to use almost every space. So, it is highly distracted by destructive anthropogenic activities. So, RESI cannot evaluate this type of urban space. Models based on historical remote sensing data and ecological indicators can be built to recommend sustainable urban growth in cities like Sylhet, one of the largest fast-growing urban hubs of Bangladesh (Rahman *et al*., 2012), and predict future ecological conditions. Evaluating the spatiotemporal evolution of ecological quality in SMA (Sylhet Metropolitan Area) from 2003 to 2023 can offer an in-depth analysis of how regional pressures related to urbanization have degraded the native ecosystem, which will benefit urban planning and improve the city's ecology for a better, sustainable, eco-friendly city (Yigitcanlar *et al*., 2015). Advanced use of remote sensing technology is a reliable medium for monitoring ecology. So, this study developed a comprehensive ecological evaluation index to integrate multisource remote sensing-based parameters to monitor changes in ecological quality over time efficiently. The study aims to evaluate spatiotemporal patterns of ecological quality between 2003 and 2023 using

Comprehensive Ecological Evaluation Index (CEEI) and identify possible causes of changing ecological quality. Understanding the future ecological condition will help the decision-maker to plan an eco-friendly, sustainable city.

2. Methodology

2.1 Study Area

The total area of Sylhet Metropolitan Area (SMA) is 26.50 sq. km and located between 24°52' and 24°55' north latitudes and between 91°50' and 91°54' east longitudes (Figure 1). Sylhet City Corporation consists of 27 wards and 192 mahallas. SMA population increased due to migration from surrounding underdeveloped villages and small towns and natural population growth. According to the 2001 Bangladesh Bureau of Statistics (BBS) census, the population of was 270606 with 1.73% growth rate (BBS, 2001). Recent estimates found that the population has significantly increased. In 2011, the population increased to 479837 with a 2.95% growth rate, and in 2022 the population increased to 532839 with a 1.03% growth rate (BBS, 2011; BBS,2022). Rapid population growth has led to the expansion of informal settlements and urban sprawl in this city (Swapan *et al*., 2016).

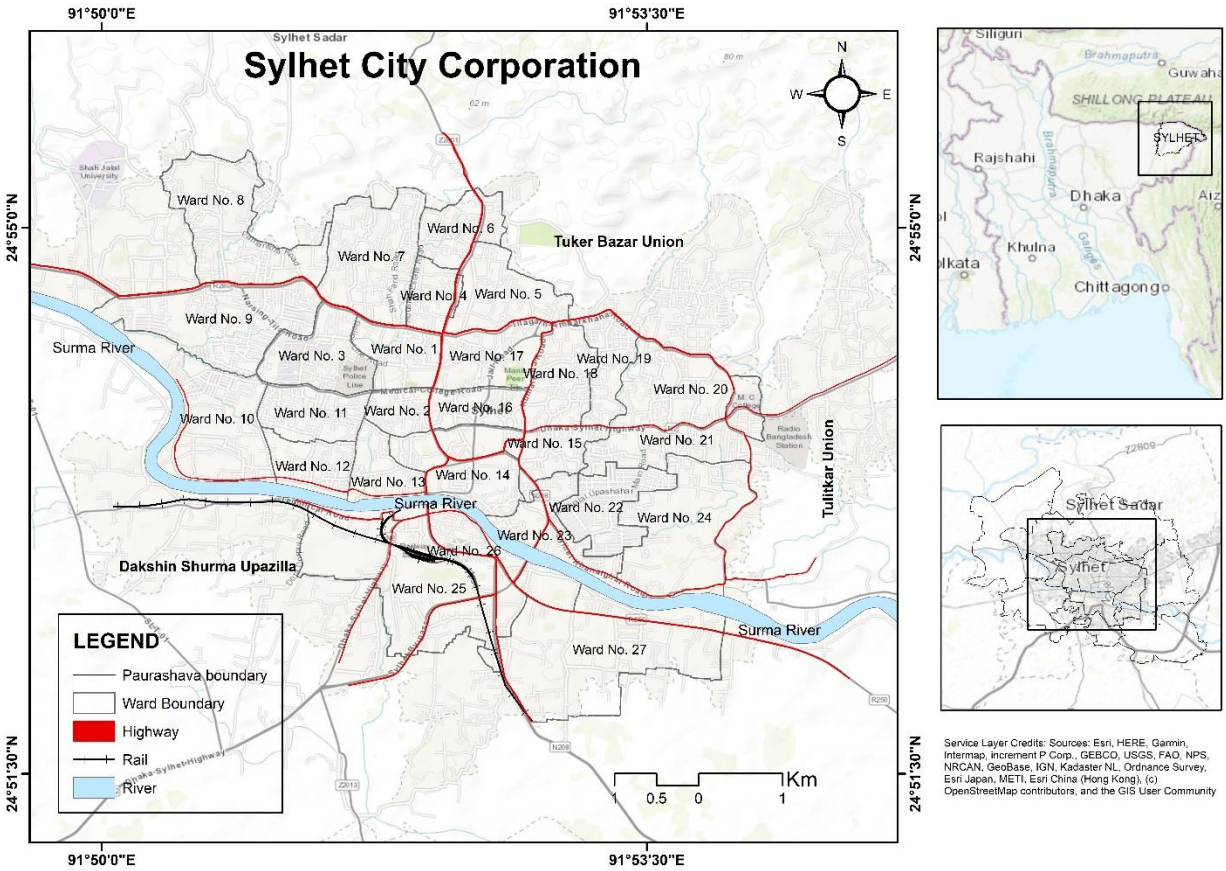

Figure 1: Geographical location of the study area

2.2 Data Collection

2.2.1 Image Data

We used Landsat images for different years to analyze temporal changes in Sylhet City Corporation. The details of the image data are presented in Table 1.

Table 1: Description of data

Year	Satellite	Sensor	Acquisition Date	Image Quality	Cloud Cover
2003	Landsat 5	Thematic Mapper (TM)	2003-01-28	9	0
2011	Landsat 5	Thematic Mapper (TM)	2011-01-10	9	0

2023	Landsat 9	Operational Land Imager (OLI)	2023-01-29	9	3.54

2.2.2 Impervious Surface Data

A cloud-based platform, Google Earth Engine (GEE), is usually used to analyze environmental data at the planetary scale. It provides numerous built-in tools and is independent of modifying and developing tools for image processing, analysis, and visualization (Tamiminia *et al*., 2020). We have used high-resolution satellite images from the Google developer's open-source dataset for remote sensing to extract footprints. The building's footprints of SMA were extracted for 2003, 2011, and 2023. To guarantee high-quality inputs for building extraction, GEE offers tools for image preprocessing, such as cloud masking, atmospheric correction, and radiometric calibration. Multi-temporal composites and mosaics can be created to reduce the effects of cloud cover and temporal variability (Gorelick *et al.,*2017). The details of the impervious data are presented in table 2.

Table 2: **Description of Impervious Data**

Year	Source	Satellite	Acquisition Date	Resolution
2023	Maxar Technologies	Airbus	22/1/2023	3m
2011	Maxar Technologies	Airbus	15/12/2011	3m
2003	Maxar Technologies	Copernicus	20/04/2003	10m

2.2.3 Model and Training Data

300 samples of building footprints of Dhaka city have been collected to train the model from the GIS Stack overflow archive(https://gis.stackexchange.com). Using Arc Map 10.8.1, the research area was extracted from the satellite image using the boundary shape file obtained from the LGED GIS Portal (https://gis.lged.gov.bd).This study accessed the ESRI Enterprise archive ArcGIS Living Atlas to obtain a trained machine-learning model for extracting building footprints from the satellite image. There are several trained models for building footprint extraction for Africa and Europe. Unfortunately, no model has been trained to extract footprints from South Asian countries. So, we selected the African Building Extraction model, a Deep Learning Package by Esri Analytics named "Building Footprint Extraction – Africa." After providing the extended

parameters and geographical data, we run the model. We have modified the model with a sample footprint from Dhaka city collected earlier. The model offers the building footprint in shape and KML file.

2.3. Data Processing and Parameter Selection

2.3.1 PSR Framework

The PSR framework is a conceptual model used to understand and manage environmental changes by linking human activities (pressure), the condition of the environment (state), and societal responses (response). Implementing this framework with remote sensing-based parameters enables the assessment of methodical environmental monitoring (Hu *et al.*, 2019).In this system 'pressure' defines human actions like pollution, urbanization, and deforestation stress the ecosystem. Whereas, 'state' represents the condition of the environment, including indicators like land cover, vegetation health, and water quality, which can be monitored using remote sensing technologies. In the PRS model, the term "response" refers to the collection of steps that administrative organizations take to mitigate the effects, such as conservation initiatives and policy implementations (Liu *et al.*, 2022)

2.3.2 CEEI Modeling

CEEI is an established and trusted method for evaluating ecosystems. Ecological indicators in CEEI can fully assess an ecosystem's health and capture intricate environmental processes. Liu *et al*. (2024) examined the extent of human impact on global ecosystems, reinforcing the need for comprehensive indices like the CEEI to account for anthropogenic pressures. Combining the PCA technique with five remote sensing-based parameters (VC, VHI, NDBSI, LSM, and LST), the CEEI was presented to characterize ecological quality. These values were carefully chosen using a framework based on pressure, status, and response (PSR) (Hughey *et al.,* 2004; Hu & Xu, 2019), which considers the idea of causation and is based on the choice and assessment of three types of factors (climate reactions, environmental conditions, and human pressures). The CEEI follows the general recommendations in academic literature (Niemi & McDonald, 2004; Seddon *et al.,* 2016). The NDBSI was used to show the degree of environmental pressure caused by human activity. Second, newly created indices of environmental states describe the current state of the environment, the quantity, quality, and quality of resources, and how they have changed over time. For this reason, VC and VHI were chosen as the parameters of the environmental state to fully identify vegetative cover and quality, respectively. Lastly, local climatic variations (temperature and humidity) in response to environmental changes were represented using the LSM and LST.

2.4 Data Analysis

2.4.1 CEEI calculation and validation

The percentage of impermeable surface covers in a given area is highly correlated with the volume of anthropogenic activities. As such, pressure intensity was taken into account using IBI. Environmental states that represent the quantity and quality of vegetation were considered using VC and VHI. Finally, climate reactions, including humidity and temperature conditions, were considered using LST and Wetness (Yang *et al.*, 2020).

$$\text{CEEI} = \text{PCA}(\text{Pressure intensity, Environmental states, Climate responses})\ldots(1)$$

In equation (1), PCA indicates the CEEI's spatial heterogeneity. All five components were normalized between 0 and 1 using the following equations: 2 and 3 to lessen the influence of climatic conditions and seasonal variations. Equ. (2) was used for LST and NDBSI (as negative values) standardization, and Equ. (3) was used for VC, VHI, and Wetness (as positive values) depending on the type of impact that each parameter had on the CEEI.

$$S_{Xi} = \frac{(X_i - X_{min})}{(X_{max} - X_{min})}\ldots(2)$$

$$S_{Xi} = \frac{(X_{max} - X_i)}{(X_{max} - X_{min})}\ldots(3)$$

The five remote sensing-based factors listed above were combined to create the CEEI, which can quickly and quantitatively assess ecological quality following Equ. (4). Here, PCA was used to determine the relative relevance of these factors and using the first component of PCA (Eq. (5)), a single-band image (also known as a CEEI image) was produced.

$$\text{CEEI} = f\,(\text{CV})\ldots(4)$$

$$\text{CEEI} = \frac{(PC1 - PC1_{min})}{(PC1_{max} - PC1_{min})}\ldots(5)$$

The CEEI values were standardized to 0–1 using Equations (2) and (3) to simplify temporal comparisons across different periods. A higher value denotes better ecological quality, while a lower one denotes poorer. Based on the CEEI mean and standard deviations, five ecological quality levels were created from the CEEI values. (Liu, 2017).

2.4.2 CEEI Classes Range from Descriptions

CEEI was classified in five different classes using the table 3.

Table 3: CEEI Classification Categories

Class	Range	Description
Excellent	0.0-0.02	No human activity exists in these places, and the vegetation there is abundant and healthy
Good	0.2-0.4	These locations have much healthy vegetation and very little human activity
Moderate	0.4-0.6	The vegetation there is mild. In these metropolitan locations, the impact of urban heat islands is not immediately apparent.
Fair	0.6-0.8	There is little vegetation and much human activity in these areas
Poor	0.8-1.0	There is very little vegetation and much human activity in these areas

2.4.3 Primary Indexing

2.4.3.1 Vegetation Cover (VC)

VC displays the vegetation distribution in a single pixel, indicating pixels with the least amount of vegetation, or soil surface with the most significant amount of vegetation, or entirely vegetation (Song *et al.*, 2017). VC is a secondary index derived from the Normalized Difference Vegetation Index (NDVI). NDVI is a metric that evaluates and quantifies the possibility of vegetation cover in the target area (Robinson *et al.*, 2017). VC value can range between 0-1. VC value of each pixel in Landsat images was calculated using the methodology suggested by Seller *et al.* (1996) (Equs. (6) and (7)).

$$\mathrm{NDVI} = \frac{(\mathrm{NIR} - \mathrm{Red})}{(\mathrm{NIR} + \mathrm{Red})} \ldots(6)$$

$$\mathrm{VC} = \frac{(\mathrm{NDVI} - \mathrm{NDVI_{soil}})}{(\mathrm{NDVIveg} - \mathrm{NDVI_{soil}})} \ldots(7)$$

2.4.3.2 Vegetative Health Index (VHI)

Three indicators were used to propose the VHI: the normalized difference vegetative index (NDVI), the normalized difference senescent vegetative index (NDSVI) (Qi *et al*., 2013), and nitrogen reflectance index (NRI) (Bausch & Duke, 1996), This can be easily derived from Landsat TM/OLI pictures and reflect the information about nitrogen, xanthophyll, and chlorophyll in vegetation, respectively. The VHI is defined as follows:

$$\text{VHI} = f\,(\text{NDVI, NRI, NDSVI}) \ldots(8)$$

$$\text{NRI} = \frac{\text{NIR}}{\text{Green}} \ldots(9)$$

$$\text{NDSVI} = \frac{\text{SWIR1- Red}}{\text{SWIR1} + \text{Red}} \ldots(10)$$

Three indicators were standardized and normalized (between 0 and 1), and then the PCA was employed to identify each variable's relative importance. As a multi-dimensional data compression tool, the PCA approach can eliminate co-linearity effects between various variables (Giannetti *et al*., 2016). Since the first PCA component's (PC1) eigenvalue integrates most of the variables' properties, PC1 was used to build the VHI in this study.

$$\text{VHI} = \frac{(\text{PC1 - PC1}_{\text{min}})}{(\text{PC1max - PC1}_{\text{min}})} \ldots(11)$$

2.4.3.3 Normalized differential build-up and bare soil index (NDBSI)

In the abandoned and deforested portions of the study area, patches of bare ground or sparsely vegetated land appeared in addition to built-up land; therefore, a soil index (SI) was applied to represent barren areas. According to Hu and Xu (2019) (Eqs. (12)–(14)):

$$\text{NDBSI} = \frac{(\text{IBI} + \text{SI})}{2} \ldots(12)$$

$$\text{IBI} = \frac{\dfrac{2\rho\text{SWIR1}}{\rho\text{SWIR1} + \rho\text{nir}} - \left[\dfrac{\rho\text{nir}}{\rho\text{nir} + \rho\text{red}} + \dfrac{\rho\text{green}}{\rho\text{green} + \rho\text{SWIR1}}\right]}{\dfrac{2\rho\text{SWIR1}}{\rho\text{SWIR1} + \rho\text{nir}} + \left[\dfrac{\rho\text{nir}}{\rho\text{nir} + \rho\text{red}} + \dfrac{\rho\text{green}}{\rho\text{green} + \rho\text{SWIR1}}\right]} \ldots(13)$$

$$\text{SI} = \frac{(\rho\text{SWIR1} + \rho\text{red}) - (\rho\text{nir} + \rho\text{blue})}{(\rho\text{SWIR1} + \rho\text{red}) + (\rho\text{nir} + \rho\text{blue})} \ldots(14)$$

2.4.3.4Land surface moisture (LSM)

LSM was calculated using the wetness component in this study (Equ. (15) and (16)).

$LSM_{TM} = 0.03151_{\rho}Blue + 0.2021_{\rho}Green + 0.3102_{\rho}Red + 0.1594_{\rho}NIR - 0.6806_{\rho}SWIR1 - 0.6109_{\rho}SWIR2$ …(15)

$LSM_{OLI} = 0.1511_{\rho}Blue + 0.1973_{\rho}Green + 0.3283_{\rho}Red + 0.3407_{\rho}NIR - 0.7117_{\rho}SWIR1 - 0.4559_{\rho}SWIR$..(16)

2.4.3.5Land surface temperature (LST)

Climate conditions may impact variations in LST throughout time and space (Weng & Fu, 2014).

$$\mathrm{LST} = \frac{\mathrm{T\ sensor}}{1 + (\lambda \times \mathrm{T\ sensor} \quad /\rho)\ \ln_e} \ldots(17)$$

where Tsensor is the at-satellite brightness temperature calculated by Eqs 18:

$$\mathrm{T\ sensor} = \frac{\mathrm{K2}}{\ln(\mathrm{K1}/\mathrm{L}\lambda + 1)} \ldots(18)$$

$$L_{\lambda} = \mathrm{Gain} \times \mathrm{DN} + \mathrm{Bias} \ldots(19)$$

Where L_{λ} is the at-sensor spectral radiance, Gain shows the band-specific multiplicative rescaling factor, and Bias indicates the band-specific additive rescaling factor. Additionally, DN indicates the digital numbers in each pixel, and *K*1 and *K*2 are the calibration coefficients for the thermal bands of TM/ETM+/OLI. For TM, ETM+ and OLI: K_2 = 1260.56 K, 1282.71 K, and 1321.08 K. K_1 = 607.76, 666.09 and 774.89 mω cm^2 (Chang *et al*., 2022).

3. Results & Discussions

3.1. Results from PCA Analysis

One of the primary objectives of this research was to identify the indicators or indices that primarily affect the urban ecology of SMA. Table 4 presents the results of the PCA analysis for three consecutive years: 2003, 2011, and 2023. Five indicative indices, e.g. VC, VHI, NDBSI, LSM, and LST, mentioned in the methodology section, were considered during the PCA Analysis.

TABLE 4: Results of the principal component analysis of each index for each year

2023	**5**	**0.0000**	**0.0000**	**100.0000**	**0.5100**	**0.1490**	**0.8430**	**0.0000**	**2.6e-003**

Year	2003					2011								
PC Layer	1	2	3	4	5	1	2	3	4	5	1	2	3	4
Eigenvalue	0.0142	0.0039	0.0036	0.0015	0.0000	142.7210	65.3112	0.4797	0.0193	0.0016	415000.0000	0.2000	0.0139	0.0003
Variance Explained(%)	61.1325	16.8651	15.5660	6.3691	0.0673	68.4405	31.3194	0.2300	0.0093	0.0008	99.9999	0.0000	0.0000	0.0000
Cumulative Variance Explained(%)	61.1325	77.9976	93.5636	99.9327	100.0000	68.4405	99.7599	99.9900	99.9992	100.0000	99.9999	100.0000	100.0000	100.0000
VC	0.7943	0.2631	-0.1461	-0.5277	-0.0011	-0.0013	0.0005	-0.0552	0.7463	0.6634	0.0000	-0.0320	0.5900	0.6100
VHI	0.6064	-0.3067	0.2380	0.6939	0.0004	-0.0015	0.0013	-0.0433	0.6620	-0.7483	0.0000	-0.0200	0.6490	0.7450
NDBSI	0.0006	-0.0005	0.0006	-0.0016	1.0000	0.9707	-0.2403	-0.0048	0.0019	-0.0004	0.0000	0.0203	-0.4700	-0.2400
LSM	-0.0150	0.8637	-0.1988	0.4630	0.0013	-0.2400	-0.9702	0.0342	0.0031	-0.0004	-0.9900	0.0004	0.0000	0.0000
LST	-0.0333	0.3014	0.9394	-0.1599	-0.0007	0.0127	0.0322	0.9969	0.0700	0.0042	0.0004	0.9900	0.0420	0.0096

For 2003, the PC1 shows the most significant values on VC and VHI, accounting for 61.13% of the variance (0.79433 and 0.60639, respectively) (Table 3). This implies that the variables that had the most impact on explaining the environmental variability in Sylhet City were VC and VHI, which are crucial for understanding urban ecological dynamics (Xiao *et al*., 2006). Furthermore, the significant role of LST in PC3 suggests that urban heat islands may have been emerging as a concern (Pan *et al.,* 2015).

By 2011, PC1 had become the most critical component in explaining environmental variability, accounting for 68.44% of the variance and significantly loading on NDBSI (0.97070), meaning urbanization has dramatically affected Sylhet City, with built-up areas emerging as the leading environmental component. LSM and NDBSI values show an inverse relationship, illustrating how land moisture typically decreases as built-up areas grow (Hu & Xu, 2019).

In 2023, the land surface moisture (-0.9990) component was the primary driver of the variance, accounting for 99.999% of the variance explained by PC1. Land surface moisture is the most crucial component influencing the environmental variability of Sylhet City in recent times. This may result from significant changes in hydrological cycles brought on by widespread urbanization or climate change (Foley *et al*., 2005).

3.2 Correlation Among the Indices

Table 5 represents the correlation matrix among the five indices mentioned in Table 4. The significant positive and negative correlation values are highlighted in the table. The environmental indices in Sylhet City in 2003 were largely independent, except VC and VHI, which had a strong positive connection (0.73634) that suggested a higher vegetation cover correlated with better vegetation health. Based on the poor correlations among the other indices, the city's environmental factors still needed to be strongly correlated. This could be because of less intense urbanization and more natural terrain. (Foody, 2002). In particular, the negative correlations involving NDBSI with both VC (-0.1367) and VHI (-0.18771) suggest that vegetation health and cover tended to decrease as built-up areas increased, reflecting the effects of urban expansion in Sylhet city.

By 2011, the interactions between various environmental indices had become more pronounced. The stronger negative correlations between LST and vegetation indices highlight the increasing importance of vegetation in mitigating urban heat (Oke, 1982).

Table 5: Correlation Matrix among VC, VHI, NDBSI, LSM and LST

			2003		
	VC	VHI	NDBSI	LSM	LST
VC	1	**0.73634**	0.01778	0.08099	-0.07379
VHI	**0.73634**	1	0.01436	-0.18377	-0.00097
NDBSI	0.01778	0.01436	1	-0.0143	0.00705
LSM	0.08099	-0.18377	-0.0143	1	0.06932
LST	-0.07379	-0.00097	0.00705	0.06932	1
			2011		
	VC	VHI	NDBSI	LSM	LST
VC	1	**0.85936**	-0.1367	0.01185	-0.30828
VHI	**0.85936**	1	-0.18771	-0.03578	-0.25461
NDBSI	-0.1367	-0.18771	1	-0.18359	0.14166
LSM	0.01185	-0.03578	-0.18359	1	-0.39121
LST	-0.30828	-0.25461	0.14166	-0.39121	1
			2023		
	VC	VHI	NDBSI	LSM	LST
VC	1	**0.87547**	**-0.98668**	0.22828	-0.27448
VHI	**0.87547**	1	-0.92699	-0.14739	-0.01749
NDBSI	**-0.98668**	**-0.92699**	1	-0.13367	0.19363
LSM	0.22828	-0.14739	-0.13367	1	-0.5027
LST	-0.27448	-0.01749	0.19363	-0.5027	1

The data from 2023 demonstrates that Sylhet City's environmental dynamics have grown more intricate and interconnected, with NDBSI and vegetation indices showing extremely high negative relationships**.** NDBSI and VC have a significant negative association (-0.98668) and VHI (-0.92699). This suggests a substantial trade-off between vegetation and built-up regions, with an increasing urban area closely linked to declining greenery. This indicates that the city's ecological

balance is seriously impacted by development, especially regarding vegetation cover and heat control. (Zhou *et al*., 2016). The crucial role that land surface moisture plays in controlling urban temperatures is highlighted by the negative correlation between LSM and LST, which should be considered when designing future metropolitan areas in light of climate change (Santamouris, 2020).

3.3 Ecological quality of SMA from 2003 to 2023

The ecological quality of SMA has been assessed with CEEI, as presented in the Figures 2 and 3. The ecological status of SMA was classified and evaluated spatiotemporally based on Table 2. Generally, Sylhet City's environmental quality showed a degradation trend from 2011 to 2023, following an improvement from 2003 to 2011. The poor and fair areas gradually shifted from suburbs to urban areas, and the ecological quality is mainly moderate, good, and excellent in 2023 (Table 6). In particular, the class with poor environmental quality had the smallest size and percentage (less than 2% of the total area) compared to the other classes.

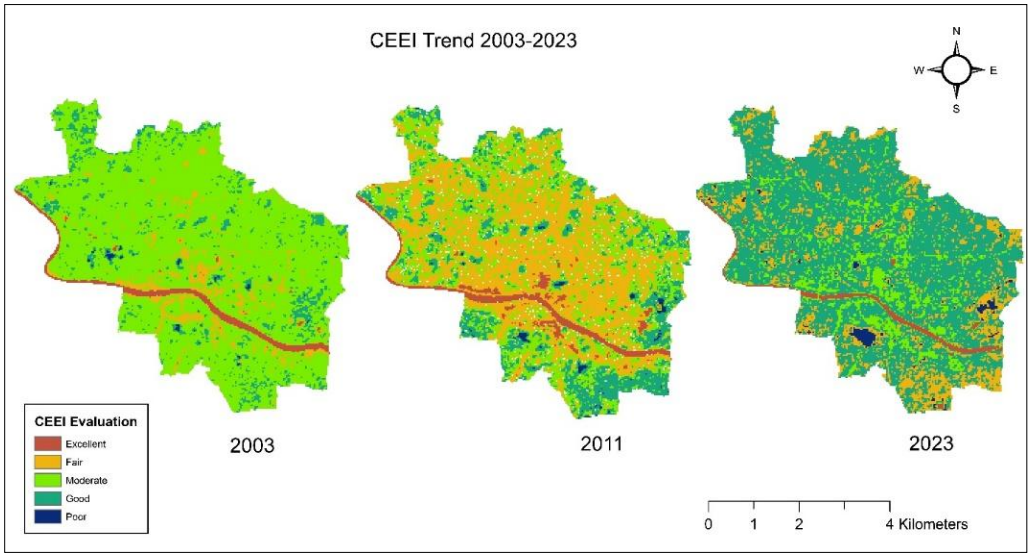

Figure 2: CEEI class classification in Sylhet City

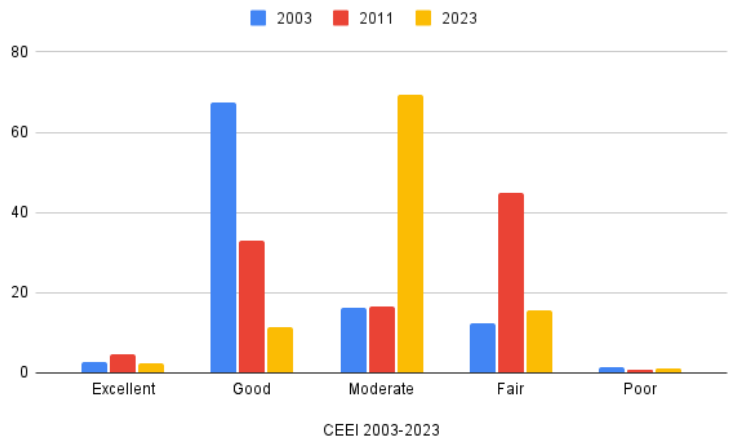

Figure 3: CEEI class classification in Sylhet City

Table 6: Area of CEEI Classification

		CEEI 2003-2023				
		Excellent	Good	Moderate	Fair	Poor
2003	Area (Acres)	169.46	4384.73	1065.93	801.06	94.96
	Percentage	2.60	67.2903	16.35	12.29	1.45
2011	Area (Acres)	312.09	2163.26	1093.19	2947.26	44.69
	Percentage	4.75	32.97	16.66	44.92	0.68
2023	Area (Acres)	162.13	762.88	4640.10	1047.65	84.41
	Percentage	2.42	11.39	69.28	15.64	1.26

For 2003, 2011, and 2023, the poor ecological quality class only had 94.96 acres (1.45%), 44.69 acres (0.68), and 84.41 (1.26%), respectively (Table 7, Fig. 3). The trend of fair ecological quality is similar to that of the poor class, both following a first downward and then upward trend (Figure 3). The area and proportion of fair quality were the largest in 2011, with 2947.26 acres (44.92%) area, and in 2023, with 1047.65 acres (15.64 %) area (Table 7, Fig 3).

There is an assessable trend throughout the 20 years from 2003 to 2023 towards a decrease in the areas classified as having the best ecological quality (Excellent and Good) and an increase in the areas classified as having moderate and poor environmental quality. In 2003, the 89.048 acres area that comprised the Excellent category accounted for 2.60% of the total area. By 2023, this area

had decreased to 162.13 acres or just 2.42% of the total. Comparably, in 2003, the good category spanned 4384.73 acres (67.29%). In addition, by 2023, that number had dropped to 762.88 acres (11.39%). On the other hand, the area under the Moderate category grew significantly between 2003 and 2023, going from 1065.93 acres (16.35%) to 4640.10 acres (62.28%) (Table 5). Even while the proportion seems to be decreasing a little, it is essential to remember that the actual area in acres is still relatively high, meaning that a large area of Sylhet City is still under moderate environmental conditions. In many South Asian cities, the amount of green space is declining while impermeable surfaces are increasing. These two factors have been linked to deteriorating environmental conditions (Ramaiah *et al*.,2019). The tendencies Sylhet City has seen fit with global trends that indicate increasing urbanization usually leads to worsening ecological quality, particularly in areas that are urbanizing quickly (Mujeri *et al*., 2020). Effective urban planning and environmental management are essential to lessen these effects and enhance the general quality of the environment in urban areas (Grimm *et al*., 2008).

3.3 Change detection of ecological quality from 2001 to 2023

The reduction in the number of regions that stay in the "Excellent" category over time may indicate an ecological regime change, in which external stressors cause ecosystems to shift from a high resilience state to a lower resilience state (Scheffer *et al*., 2001). Degradation of places from Excellent to Lower conditions may also be associated with declining ecosystem services and biodiversity, which are essential for preserving ecological balance and human welfare. (Cardinale *et al*., 2012). The changes in ecological quality between 2003 and 2023 are presented in Table 7 as a transition matrix. The magnitude of the changes is calculated using the transition matrix and shown in Table 8 and in Figure 4 thematically.

Table 7: CEEI Quality Transition in SMA

		T_1				
		Excellent	**Good**	**Moderate**	**Fair**	**Poor**
T_2	**Excellent**	Unchanged	Improved	Improved	Improved	Improved
	Fair	Degraded	Unchanged	Improved	Improved	Improved
	Good	Degraded	Degraded	Unchanged	Improved	Improved
	Moderate	Degraded	Degraded	Degraded	Unchanged	Improved
	Poor	Degraded	Degraded	Degraded	Degraded	Unchanged

Table 8: CEEI Transition in percent

	2003-2023				
	Excellent	**Good**	**Moderate**	**Fair**	**Poor**
Excellent	90.48	0.85	1.88	6.00	0.79
Fair	0.18	79.93	16.55	3.03	0.31
Good	0.13	1.84	95.48	2.27	0.27
Moderate	0.26	0.88	59.12	37.07	2.67
Poor	0.46	11.95	10.27	10.80	66.51

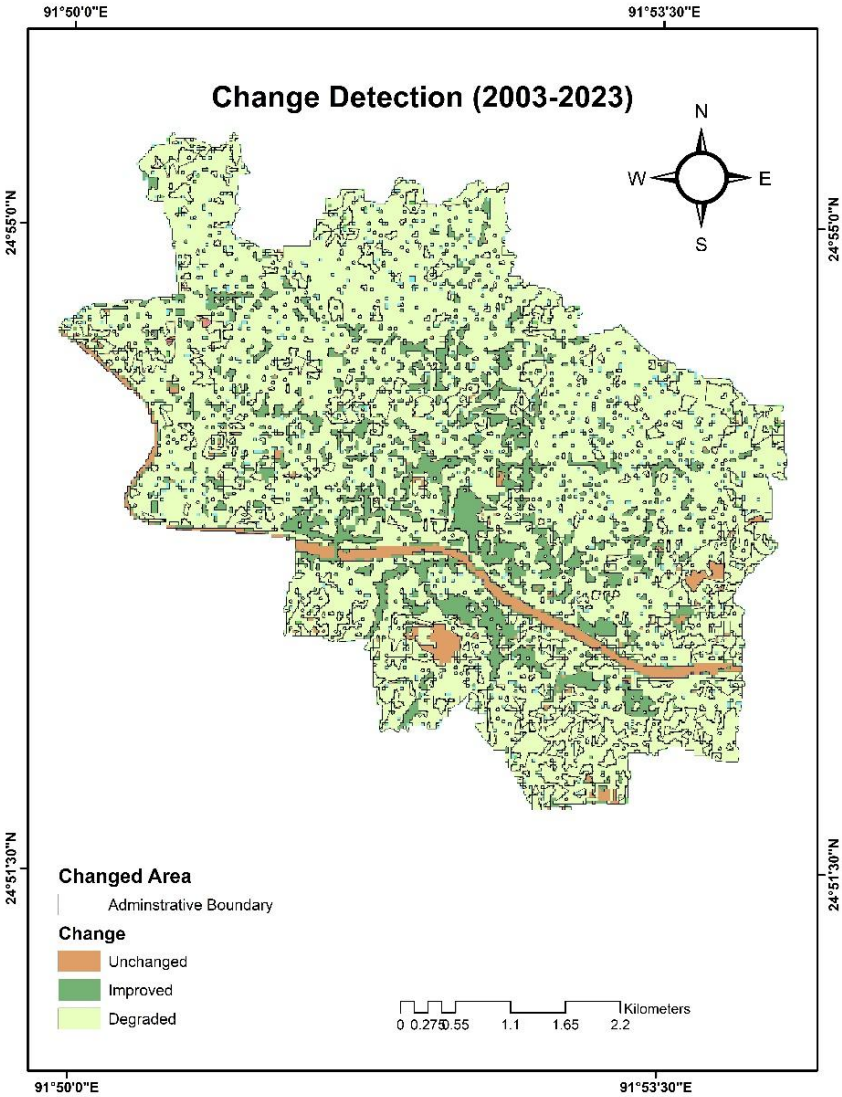

Figure 4: Change dynamics of Sylhet City from 2003 to 2023

The strong persistence of excellent are

as is indicated by the high percentage (76.41%) of areas that transitioned from "Excellent" to "Excellent" in the initial period. Nevertheless, this proportion falls to 57.87% in the second period (2011–2023), reducing these areas' capacity to hold their original state. The percentage of "Fair" locations that move to "Fair" also significantly decreases, from 72.90 percent to 19.83 percent, suggesting that these places are under increasing pressure. There is a noticeable rise in areas dropping from higher categories (Excellent, Fair, and Good) to lower categories (Moderate, Poor). For example, the percentage of "Fair" areas that changed to "Poor" in the second period rose from 2.55 to 4.58 percent. Areas recognized as "Moderate" or "Poor" in 2011 and improved in 2023. For instance, the percentage of "Poor" locations that became "Good" rose from 7.65 percent to 11.99 percent.

In the years 2003 -2011, the ecological quality degraded from moderate class to poor class (32.26%), good class to moderate class (32.90%), and fair class to poor class (30.24%) respectively. Furthermore, a small area improved from poor class to moderate class (3.77%)and fair class to good class (47.10%).

In the second transition period (2011-2023) ecological quality degraded more from moderate to fair class (40.63), good to fair class (77.55), and good to moderate class (42.93) respectively. Moreover, improved areas consist of small portions from poor to moderate class (2.62%) and fair to excellent class (38.84%) respectively.

Several contributing factors to the degradation of the ecological quality in the region. According to the Global Forest Watch (GFW), the Sylhet region lost 5,523 hectares of tree cover, reserved forests, and protected areas from 2001 to 2012. For example, Lawachara reserved forests lost 1,188 trees in 2005-2006)(Roy et al ., 2006). The climatic data of the average annual rainfall in Sylhet has revealed a decrease while the average annual temperature has revealed an increase from 1999 to 2011, and the mean annual rainfall was less than the normal range i.e. 4195.9 mm)(Choudhury et al ., 2012). However, the current infrastructural development process and the highest deficit in rainfall in Sylhet induced the deterioration of the ecological quality (Hoque et al ., 2022).

Transitions from the "Moderate" group to the "Poor" category increased significantly in the later period (from 32.26 percent to 40.63 percent).

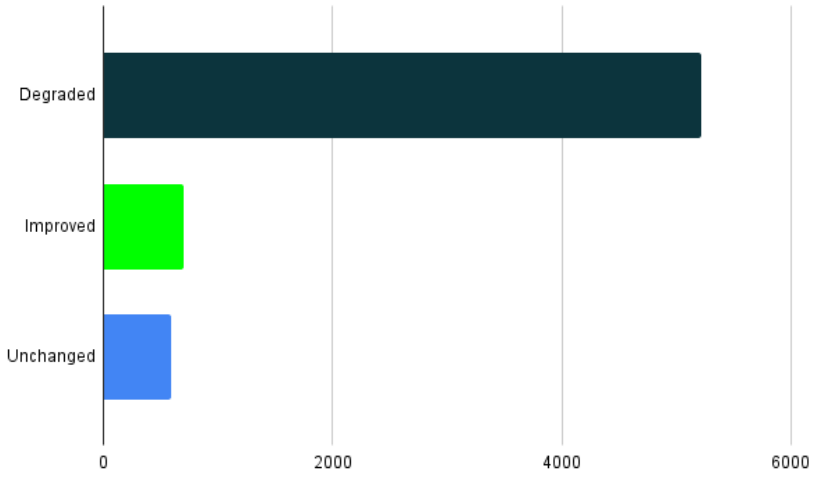

Figure 5: CCEI changes in Sylhet city during the three study years (ha)

Figure 5 shows that most of the land's quality was the same during the study period, and there is a noticeable recovery process. Unfortunately, the degradation was far higher than the recovery rate. So, there was a significant degradation during the last 20 years.

From 2003 to 2011 and 2011 to 2023, the continuous growth of degraded categories indicates the city's continuously degrading ecological condition. These trends are similar to urban growth worldwide, where fast urbanization frequently results in higher pollution, the loss of vegetation, and deteriorating air and water quality (Seto *et al*., 2012).

Ecological quality degradation seen in Sylhet City is consistent with other issues that many cities across the world are facing. Environmental degradation is usually the result of urban growth, especially in quickly expanding cities where the demand for resources and land might exceed the ability for sustainable management (Angel *et al*., 2011). Increased impermeable surfaces, less vegetation cover, and higher pollution emissions are all consequences of urbanization that lead to environmental degradation (Bai *et al*., 2020).

Bangladesh introduced several strict urban planning policies and environmental protection laws, which may have been responsible for the initial improvement from 2003 to 2011. However, more than the policy was needed for ecological restoration in the long run. This pattern shows that ongoing human pressures have the power to reverse ecological restoration's short-term successes (Hobbs *et al*., 2009).

3.4 Urban Settlement Expansion Pattern

In this study, the urban expansion of SMA was analyzed by examining the growth of settlements over time. Figure 6 shows the spatial distribution of urban expansion patches in Sylhet city in between 2003 and 2023. The findings revealed that the urban settlement area was 3.30 km^2 in 2003, which expanded to 6.91 km^2 by 2023, indicating around a 3.63 km^2 increase in urban settlement area (Table 9). This urban growth signified 86.16% of edge expansion, 12.64% of outlying expansion, and 1.20% infilling from 2003 to 2023 in Sylhet City. The following result showed that edge expansion patches were more prominent than outlying and infilling patches. Furthermore, edge expansion was noticed all over the area, and outlying patches are primarily observed in the northern, southern, and southeastern directions. These three landscape expansion patterns indicate urban fragmentation. Additionally, a high percentage of edge expansion patches indicate the gradual increase of urban areas from undeveloped areas (Tian *et al*., 2022).

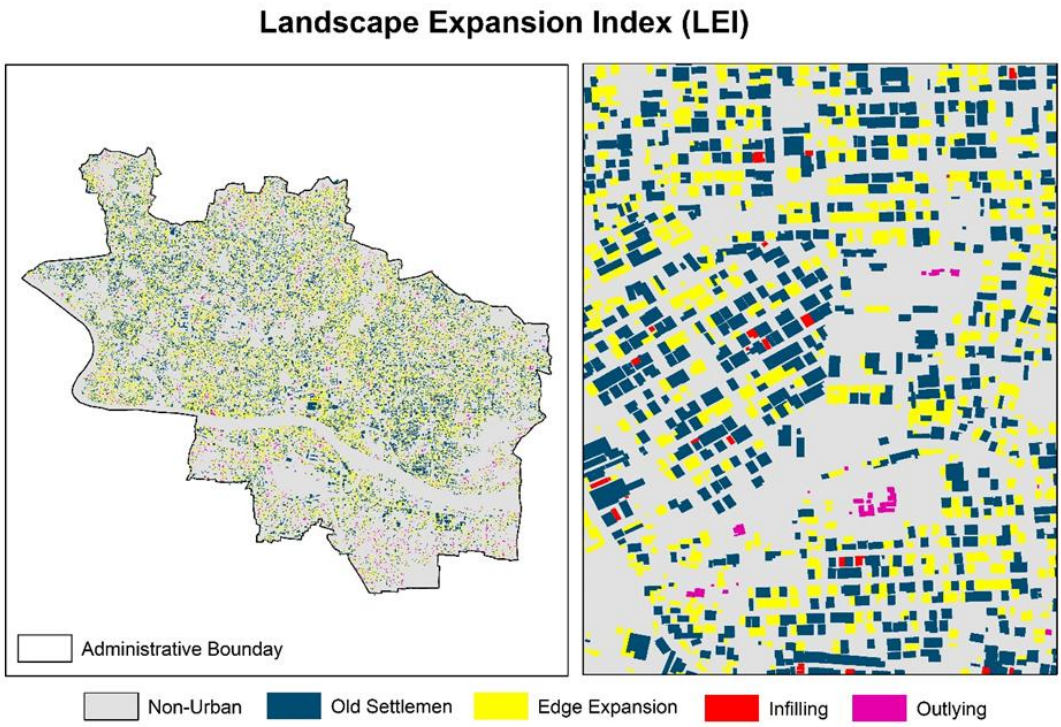

Figure 6: Spatial distribution of urban landscape expansion patterns in Sylhet City from 2003 to 2023

Table 9: Area of three landscape expansion patterns from 2003 to 2023

New patches	Area of new patches (Km^2)	Percentage

Infilling	0.04	1.20
Edge Expansion	3.13	86.16
Outlying	0.46	12.64
Total	3.62	100.00

4. Conclusion

The ecological quality of SMA was evaluated by using satellite imagery from 2003 to 2023 and integrating the Comprehensive Ecological Evolution Index(CEEI). The result revealed that the ecological quality degraded over time with urban growth. Though there is a slight improvement during 2003-2011 because of high-rise buildings and the reduction of urban sprawl. However, from 2011 to 2023, the ecological quality was not positive due to rapid migration and simultaneous growth rates, with the increases rates of fair and poor ecological quality classes and the decrease rates with excellent and good ecological quality classes. The SMA faces great challenges and threatens regional development through ecological preservation and conservation. CEEI can be an affordable alternative for SMA's long-term ecological monitoring. The outcomes of the study will help policymakers and provide positive insight into the decision-making process. In future studies, the uneven elevation of Sylhet City can create more valuable insight using TPI masking, and due to the different nature of the waterbody and plain land, they should be addressed using the distinct models for each to avoid biased weight classification of indices.

Funding statement

This research received no specific grant from funding agencies in the public, commercial, or not-for-profit sectors.

Data availability statement

All data used in this study are fully available within the manuscript.

Declaration of competing interest

The authors declare that they have no known competing financial interests or personal relationships that could have appeared to influence the work reported in this paper.

Acknowledgments

We are grateful to the BBS of GoB, and USGS, NASA Power team for facilitating easy access to information. We also express our heartfelt thanks to the faculty and students of the Dept. of Geography and Environment, Islamic University, Kushtia 7003, Bangladesh for the utmost assistance and support throughout the study.

References

Abdullah, S., Adnan, M. S. G., Barua, D., Murshed, M. M., Kabir, Z., Chowdhury, M. B. H., ... & Dewan, A. (2022). Urban green and blue space changes: A spatiotemporal evaluation of impacts on ecosystem service value in Bangladesh. *Ecological Informatics*, *70*, 101730.

Ahsan, R., Kellett, J., & Karuppannan, S. (2016). Climate migration and urban changes in Bangladesh. In *Urban disasters and resilience in Asia* (pp. 293-316). Butterworth-Heinemann.

Angel, S., Parent, J., Civco, D. L., Blei, A., & Potere, D. (2011). The dimensions of global urban expansion: Estimates and projections for all countries, 2000–2050. *Progress in planning*, *75*(2), 53-107.

Austin, M. (2007). Species distribution models and ecological theory: a critical assessment and some possible new approaches. *Ecological modelling*, *200*(1-2), 1-19.

Ba, R., Song, W., Li, X., Xie, Z., & Lo, S. (2019). Integration of multiple spectral indices and a neural network for burned area mapping based on MODIS data. *Remote Sensing*, *11*(3), 326.

Bai, X., Nagendra, H., Shi, P., & Liu, H. (2020). Cities: Build networks and share plans to emerge stronger from COVID-19. *Nature*, *584*(7822), 517-520.

Baig, M. H. A., Zhang, L., Shuai, T., & Tong, Q. (2014). Derivation of a tasselled cap transformation based on Landsat 8 at-satellite reflectance. *Remote Sensing Letters*, *5*(5), 423–431.

Bangladesh Bureau of Statistics. (2011). *Population and housing census 2011*. Ministry of Planning, Government of Bangladesh.

Bangladesh Bureau of Statistics. (2023). *Population and housing census 2011*. Ministry of Planning, Government of Bangladesh.

Bausch, W. C., & Duke, H. R. (1996). Remote sensing of plant nitrogen status in corn. *Transactions of the ASAE*, *39*(5), 1869-1875.

Cardinale, B. J., Duffy, J. E., Gonzalez, A., Hooper, D. U., Perrings, C., Venail, P., ... & Naeem, S. (2012). Biodiversity loss and its impact on humanity. *Nature*, *486*(7401), 59–67.

Chang, Y., Xiao, J., Li, X., Zhou, D., & Wu, Y. (2022). Combining GOES-R and ECOSTRESS land surface temperature data to investigate diurnal variations of surface urban heat island. *Science of The Total Environment*, *823*, 153652.

Choudhury, S. A., Terao, T., Murata, F., & Hayashi, T. (2012). Seasonal variations of temperature and rainfall characteristics in the northeastern part of Bangladesh around Sylhet. *J Agrofor Environ*, *6*(2), 81-88.

Crist, E. P. (1985). A TM tasseled cap equivalent transformation for reflectance factor data. *Remote sensing of Environment*, *17*(3), 301–306.

Du, C., Ren, H., Qin, Q., Meng, J., & Zhao, S. (2015). A practical split-window algorithm for estimating land surface temperature from Landsat 8 data. *Remote sensing*, *7*(1), 647-665.

Fern, R. R., Foxley, E. A., Bruno, A., & Morrison, M. L. (2018). Suitability of NDVI and OSAVI as estimators of green biomass and coverage in a semi-arid rangeland. *Ecological Indicators*, pp. *94*, 16–21.

Firozjaei, M. K., Sedighi, A., Mijani, N., Kazemi, Y., & Amiraslani, F. (2023). Seasonal and daily effects of the sea on the surface urban heat island intensity: A case study of cities in the Caspian Sea Plain. *Urban Climate*, *51*, 101603.

Foley, J. A., DeFries, R., Asner, G. P., Barford, C., Bonan, G., Carpenter, S. R., ... & Snyder, P. K. (2005). Global consequences of land use. *science*, *309*(5734), 570-574.

Foody, G. M. (2002). Status of land cover classification accuracy assessment. *Remote sensing of environment*, *80*(1), 185–201.

Geng, J., Yu, K., Xie, Z., Zhao, G., Ai, J., Yang, L., ... & Liu, J. (2022). Analysis of spatiotemporal variation and drivers of ecological quality in Fuzhou based on RSEI. *Remote Sensing*, *14*(19), 4900.

Giannetti, C., Ransing, R. S., Ransing, M. R., Bould, D. C., Gethin, D. T., & Sienz, J. (2014). A novel variable selection approach based on co-linearity index to discover optimal process settings by analysing mixed data. *Computers & Industrial Engineering*, *72*, 217-229.
Giannetti, C., Ransing, R. S., Ransing, M. R., Bould, D. C., Gethin, D. T., & Sienz, J. (2014). A novel variable selection approach based on co-linearity index to discover optimal process settings by analysing mixed data. *Computers & Industrial Engineering*, *72*, 217-229.
Gorelick, N., Hancher, M., Dixon, M., Ilyushchenko, S., Thau, D., & Moore, R. (2017). Google Earth Engine: Planetary-scale geospatial analysis for everyone. *Remote sensing of Environment*, pp. *202*, 18–27.

Grimm, N. B., Faeth, S. H., Golubiewski, N. E., Redman, C. L., Wu, J., Bai, X., & Briggs, J. M. (2008). Global change and the ecology of cities. *science*, *319*(5864), 756-760.

Hobbs, R. J., Higgs, E., & Harris, J. A. (2009). Novel ecosystems: implications for conservation and restoration. *Trends in ecology & evolution*, *24*(11), 599–605.

Hoque, M. J. (2022). Causes, mechanisms and outcomes of environmental degradation in bangladesh: a study in sylhet.DOI:10.5109/4793670

Hossain, M. S. (2018). Urban growth and land use change detection using remote sensing and GIS techniques: A case study of Sylhet City Corporation, Bangladesh. Environmental Challenges, 3, 100018. https://doi.org/10.1016/j.envc.2018.07.001

Hu, X. J., Xu, H. Q., Guo, Y. B., & Zhang, B. B. (2017). Remote sensing detection of vegetation health status after ecological restoration in soil and water loss region. *Ying Yong Sheng tai xue bao= The Journal of Applied Ecology*, *28*(1), 250–256.

Hu, X., & Xu, H. (2019). A new remote sensing index based on the pressure-state-response framework to assess regional ecological change. *Environmental Science and Pollution Research*, pp. *26*, 5381–5393.

Hughey, K. F. D., Cullen, R., & Moran, E. (2004). Integrating economics into priority setting and evaluation in conservation management. Conservation Biology, 17(1), 274-287

Hunsaker, C. T., & Hughes, R. M. (2002). Effects of landscape change on the physical and chemical components of aquatic ecosystems. In *Applying landscape ecology in biological conservation* (pp. 286–308). New York, NY: Springer, New York.

Islam, M. N., Sarker, S. K., & Mustafa, M. G. (2020). Urbanization and its impact on biodiversity: A case study on Sylhet City Corporation, Bangladesh. Journal of Urban Ecology, 6(1), juaa014. https://doi.org/10.1093/jue/juaa014

Kadir, A., Ahmed, Z., Uddin, M. M., Xie, Z., & Kumar, P. (2021). An integrated approach to quantify the impact of land use and land cover changes on water quality of Surma River, Sylhet, Bangladesh. *Water*, *14*(1), 17.

Liu, F.P., (2017). Evaluation of Ecological Environment in Songhua River Basin based on RS and GILiu, X., Zhang, Z., Li, M., Fu, Y., & Hui, Y. (2022). Ecological source identification based on the PSR model framework and structural features: a case study in Tianjin, China. *Arabian Journal of Geosciences*, *15*(9), 853.

Liu, H., Pang, S., Sun, M., Liu, J., & Li, Q. (2024). How can small and medium-sized cities differentiate their carbon peaks?. *Ecological Indicators*, *158*, 111231.

Liu, X., Zhang, Z., Li, M., Fu, Y., & Hui, Y. (2022). Ecological source identification based on the PSR model framework and structural features: a case study in Tianjin, China. *Arabian Journal of Geosciences*, *15*(9), 853.

Liu, Y., Xu, J., & Luo, H. (2014). An integrated approach to modelling the economy-society-ecology system in urbanization process. *Sustainability*, *6*(4), 1946-1972.

Luo, D., Jin, H., Marchenko, S. S., & Romanovsky, V. E. (2018). Difference between near-surface air, land surface and ground surface temperatures and their influences on the frozen ground on the Qinghai-Tibet Plateau. *Geoderma*, *312*, 74-85.

Mas, J. F., Pérez-Vega, A., & Clarke, K. C. (2014). Assessing simulated land use/cover maps using landscape metrics. Ecological Indicators, 38, 102111.

Mujeri, M. K., Mujeri, N., Mujeri, M. K., & Mujeri, N. (2020). Social and Climate Change Vulnerability. *Bangladesh at Fifty: Moving beyond Development Traps*, 377-444.

Niemi, G. J., & McDonald, M. E. (2004). Application of ecological indicators. *Annu. Rev. Ecol. Evol. Syst.*, *35*(1), 89-111.

Oke, T. R. (1982). The energetic basis of the urban heat island. *Quarterly journal of the royal meteorological society*, *108*(455), 1–24.

Pan, J. (2015). Analysis of human factors on urban heat island and simulation of urban thermal environment in Lanzhou city, China. *Journal of Applied Remote Sensing*, *9*(1), 095999-095999.

Qi, J., Marsett, R., Heilman, P., Bieden-bender, S., Moran, S., Goodrich, D., & Weltz, M. (2002). RANGES improve satellite-based information and land cover assessments in the southwest United States. *Eos, Transactions American Geophysical Union*, *83*(51), 601-606.

Rahman, A., Khan, K., Krakauer, N. Y., Roytman, L., & Kogan, F. (2012). Use of remote sensing data for estimation of Aman rice yield. *Int. J. Agric. For*, *2*(1), 101-107.

Rahman, M. M., & Alam, M. J. B. (2016). Impact of land use change on the ecosystem services of Sylhet City Corporation. Asian Journal of Water, Environment, and Pollution, 13(2), 31-39. https://doi.org/10.3233/AJW-160022

Ramaiah, M., & Avtar, R. (2019). A review of urban green spaces and their need in cities of rapidly urbanizing India. *Urban science*, *3*(3), 94.

Robinson, N. P., Allred, B. W., Jones, M. O., Moreno, A., Kimball, J. S., Naugle, D. E., ... & Richardson, A. D. (2017). A dynamic Landsat-derived normalized difference vegetation index (NDVI) product for the conterminous United States. *Remote sensing*, *9*(8), 863.

Roy, M. K., & DeCosse, P. (2006). Managing demand for protected areas in Bangladesh: poverty alleviation, illegal commercial use and nature recreation. *Policy Matters*, *14*, 93-102.

Santamouris, M. (2020). Recent progress on urban overheating and heat island research. Integrated assessment of the energy, environmental, vulnerability, and health impact. Synergies with the global climate change. *Energy and Buildings*, *207*, 109482.

Scheffer, M., Carpenter, S., Foley, J. A., Folke, C., & Walker, B. (2001). Catastrophic shifts in ecosystems. *Nature*, *413*(6856), 591–596.

Seddon, A. W., Macias-Fauria, M., Long, P. R., Benz, D., & Willis, K. J. (2016). Sensitivity of global terrestrial ecosystems to climate variability. *Nature*, *531*(7593), 229-232.

Sellers, P. J., Tucker, C. J., Collatz, G. J., Los, S. O., Justice, C. O., Dazlich, D. A., & Randall, D. A. (1996). A revised land surface parameterization (SiB2) for atmospheric GCMs. Part II: The generation of global fields of terrestrial biophysical parameters from satellite data. *Journal of Climate*, *9*(4), 706-737.

Seto, K. C., Güneralp, B., & Hutyra, L. R. (2012). Global forecasts of urban expansion to 2030 and direct impacts on biodiversity and carbon pools. *Proceedings of the National Academy of Sciences*, *109*(40), 16083-16088.

Seto, K. C., Güneralp, B., & Hutyra, L. R. (2012). Global forecasts of urban expansion to 2030 and direct impacts on biodiversity and carbon pools. *Proceedings of the National Academy of Sciences*, *109*(40), 16083-16088.

Sobrino, J. A., Jiménez-Muñoz, J. C., & Paolini, L. (2004). Land surface temperature retrieval from LANDSAT TM 5. *Remote Sensing of Environment*, *90*(4), 434-440.

Song, H. M., & Xue, L. (2016). Dynamic monitoring and analysis of the ecological environment in Weinan City, Northwest China, based on the RSEI model. *Ying Yong sheng tai xue bao= The Journal of Applied Ecology*, *27*(12), 3913-3919.

Song, W., Mu, X., Ruan, G., Gao, Z., Li, L., & Yan, G. (2017). Estimating fractional vegetation cover and the vegetation index of bare soil and highly dense vegetation with a physically based method. *International journal of applied earth observation and geoinformation*, *58*, 168-176.

Swapan, M. S. H., Zaman, A. U., Ahsan, T., & Ahmed, F. (2017). Transforming urban dichotomies and challenges of South Asian megacities: Rethinking sustainable growth of Dhaka, Bangladesh. *Urban Science*, *1*(4), 31.

Tamiminia, H., Salehi, B., Mahdianpari, M., Quackenbush, L., Adeli, S., & Brisco, B. (2020). Google Earth Engine for geo-big data applications: A meta-analysis and systematic review. *ISPRS journal of photogrammetry and remote sensing*, *164*, 152-170.

Tian, Y., Shuai, Y., Ma, X., Shao, C., Liu, T., & Tuerhanjiang, L. (2022). Improved landscape expansion index and its application to urban growth in urumqi. *Remote Sensing*, *14*(20), 5255, https://doi.org/10.3390/rs14205255

Voogt, J. A., & Oke, T. R. (2003). Thermal remote sensing of urban climates. *Remote sensing of environment*, *86*(3), 370-384.

Walker, B., Holling, C. S., Carpenter, S. R., & Kinzig, A. (2004). Resilience, adaptability, and transformability in social-ecological systems. *Ecology and Society*, *9*(2).

Weng, Q., & Fu, P. (2014). Modeling annual parameters of clear-sky land surface temperature variations and evaluating the impact of cloud cover using a time series of Landsat TIR data. *Remote Sensing of Environment*, *140*, 267-278.

Xiao, X., Hagen, S., Zhang, Q., Keller, M., & Moore III, B. (2006). Detecting leaf phenology of seasonally moist tropical forests in South America with multi-temporal MODIS images. *Remote Sensing of Environment*, *103*(4), 465-473.

Xu, F., Hu, C., Li, J., Plaza, A., & Datcu, M. (2020). Special focus on deep learning in remote sensing image processing. *Science China. Information Sciences*, *63*(4), 140300.

Yang, F., Pang, B., Song, L., Cheng, H., Zhou, S., Zheng, Z., ... & Zuo, D. (2024). Response of extreme precipitation to urban expansion over the Guangdong-Hong Kong-Macao Greater Bay Area. *Urban Climate*, *56*, 102062.

Yang, H., Li, W., Wang, S., Li, H., Guan, J., Zhou, S., & Cao, J. (2023). Spatial-Temporal Data Mining for Ocean Science: Data, Methodologies, and Opportunities. *arXiv preprint arXiv:2307.10803*.

Yang, Y., Zhang, M., Li, Q., Chen, B., Gao, Z., Ning, G., ... & Luo, M. (2020). Modulations of surface thermal environment and agricultural activity on intraseasonal variations of summer diurnal temperature range in the Yangtze River Delta of China. *Science of The Total Environment*, *736*, 139445.

Yi, Y., Zhang, Z., Zhang, W., Zhang, C., Li, W., & Zhao, T. (2019). Semantic segmentation of urban buildings from VHR remote sensing imagery using a deep convolutional neural network. *Remote sensing*, *11*(15), 1774.

Yigitcanlar, T., & Teriman, S. (2015). Rethinking sustainable urban development: towards an integrated planning and development process. *International journal of environmental science and technology*, *12*, 341-352.

Yu, Z., Yao, Y., Yang, G., Wang, X., & Vejre, H. (2019). Rapid urbanization and urban agglomeration development substantially contribute to regional thermal environment dynamics and evolution. *Forest Ecology and Management*, *446*, 214-225.

Zhou, D., Zhang, L., Hao, L., Sun, G., Liu, Y., & Zhu, C. (2016). Spatiotemporal trends of urban heat island effect along China's urban development intensity gradient. *Science of the Total Environment*, pp. *544*, 617–626.

Zhu, S., Cui, N., Guo, L., Jin, H., Jin, X., Jiang, S., ... & Wang, M. (2024). Enhancing precision of root-zone soil moisture content prediction in a kiwifruit orchard using UAV multi-spectral image features and ensemble learning. *Computers and Electronics in Agriculture*, *221*, 108943.